Mombers, C., Verkleij, A. J., De Gier, J., & van Deenen, L. L. M. (1979) *Biochim. Biophys. Acta 551*, 271–281.
Op den Kamp, J. A. F. (1979) *Annu. Rev. Biochem. 48*, 47–71.
Rosing, J., van Rijn, J. L. M., Bevers, E. M., van Dieijen, G., Comfurius, P., & Zwaal, R. F. A. (1985) *Blood 65*, 319–332.
Rybicki, A. C., Heath, R., Lubin, B., & Schwartz, R. S. (1988) *J. Clin. Invest. 81*, 255–260.
Schick, P. K., Kurica, K. B., & Chacko, G. K. (1976) *J. Clin. Invest. 57*, 1221–1226.
Schroit, A. J., Madsen, J. W., & Tanaka, Y. (1985) *J. Biol. Chem. 260*, 5131–5138.
Schwartz, R. S., Tanaka, Y., Fidler, I. J., Chiu, D., Lubin, B., & Schroit, A. J. (1985) *J. Clin. Invest. 75*, 1965–1973.
Seigneuret, M., & Devaux, P. F. (1984) *Proc. Natl. Acad. Sci. U.S.A. 81*, 3751–3755.
Seigneuret, M., Zachowski, A., Herrmann, A., & Devaux, P. F. (1984) *Biochemistry 23*, 4271–4275.
Spangenberg, P., Till, U., Gschmeissner, S., & Crawford, N. (1987) *Br. J. Haematol. 67*, 443–450.
Sune, A., Bette-Bobillo, P., Bienvenue, A., Fellmann, P., & Devaux, P. F. (1987) *Biochemistry 26*, 2972–2978.
Tanaka, Y., & Schroit, A. J. (1983) *J. Biol. Chem. 258*, 11335–11343.
Tilley, L., Cribier, S., Roelofsen, B., Op den Kamp, J. A. F., & van Deenen, L. L. M. (1986) *FEBS Lett. 194*, 21–27.
Verhallen, P. F. J. (1988) Ph.D. Thesis, University of Limburg.
Verhallen, P. F. J., Bevers, E. M., Comfurius, P., & Zwaal, R. F. A. (1987) *Biochim. Biophys. Acta 903*, 206–217.
Verhallen, P. F. J., Bevers, E. M., Comfurius, P., & Zwaal, R. F. A. (1988) *Biochim. Biophys. Acta 952*, 150–158.
Verkleij, A. J., Zwaal, R. F. A., Roelofsen, B., Comfurius, P., Kastelijn, D., & van Deenen, L. L. M. (1973) *Biochim. Biophys. Acta 323*, 178–193.
Williamson, P., Antia, R., & Schlegel, R. A. (1987) *FEBS Lett. 219*, 316–320.
Wroblewski, R., & La Due, J. S. (1955) *Proc. Soc. Exp. Biol. Med. 90*, 210–215.
Zachowski, A., Favre, E., Cribier, S., Herve, P., & Devaux, P. F. (1986) *Biochemistry 25*, 2585–2590.
Zachowski, A., Herrmann, A., Paraf, A., & Devaux, P. F. (1987) *Biochim. Biophys. Acta 897*, 197–200.
Zwaal, R. F. A., Roelofsen, B., Comfurius, P., & van Deenen, L. L. M. (1975) *Biochim. Biophys. Acta 406*, 83–96.

Heteronuclear Three-Dimensional NMR Spectroscopy of the Inflammatory Protein C5a

Erik R. P. Zuiderweg* and Stephen W. Fesik

Pharmaceutical Discovery Division, D47G, AP9, Abbott Laboratories, Abbott Park, Illinois 60064

Received December 15, 1988

ABSTRACT: The utility of three-dimensional heteronuclear NMR spectroscopy for the assignment of ^{1}H and ^{15}N resonances of the inflammatory protein C5a (MW 8500), uniformly labeled with ^{15}N, is demonstrated at a protein concentration of 0.7 mM. It is shown that dramatic simplification of the 2D nuclear Overhauser effect spectrum (NOESY) is obtained by editing with respect to the frequency of the ^{15}N heteronucleus in a third dimension. The improved resolution in the 3D experiment largely facilitates the assignment of protein NMR spectra and allows for the determination of distance constraints from otherwise overlapping NOE cross peaks for purposes of 3D structure determination. The results show that ^{15}N heteronuclear 3D NMR can facilitate the structure determination of small proteins and promises to be a useful tool for the study of larger systems that cannot be studied by conventional 2D NMR techniques.

The determination of three-dimensional structures of small proteins in solution by high-resolution NMR spectroscopy has become a well established technique. The method relies on the identification of a large number of internuclear distance constraints obtained from nuclear Overhauser effects (NOEs),[1] which are used to calculate an ensemble of tertiary structures [for a review, see Wüthrich (1986)]. Thus far, 3D structure determinations by NMR have been limited to relatively small proteins of a molecular weight smaller than 10000. This size limitation is due to the difficulty in assigning the NOE cross peaks in two-dimensional (2D) NOE spectroscopy data (NOESY) to specific proton pairs in larger proteins because of the vast number of overlapping signals. In order to determine the structures of larger proteins by NMR, novel NMR techniques need to be developed to resolve this problem of spectral overlap.

Recently, we and others (Fesik & Zuiderweg, 1988; Bax et al., 1988) have proposed the use of heteronuclear three-dimensional (3D) NMR spectroscopy for the simplification of NMR spectra of larger systems. The 3D experiments are combinations of homonuclear 2D NMR experiments [for a review, see Ernst et al. (1987)] such as NOESY and COSY and heteronuclear multiple quantum correlation (HMQC) (Müller, 1979; Bax et al., 1984) techniques. Heteronuclear 3D NMR has the advantage over homonuclear 3D NMR (Vuister & Boelens, 1987; Griesinger et al., 1987a,b; Oschkinat et al., 1988; Vuister et al., 1988) in that one of the coherence transfer steps involves the heteronuclear scalar coupling which is large compared to the ^{1}H line width, allowing high sensitivity even when these experiments are applied to large molecules.

[1] Abbreviations: NOE, nuclear Overhauser effect; 1D, one dimensional; 2D, two dimensional; 3D, three dimensional; NOESY, 2D NOE spectroscopy; HMQC, 2D heteronuclear multiple quantum correlation.

0006-2960/89/0428-2387$01.50/0

Experimental verification of heteronuclear 3D NMR has recently been described by using a ^{15}N-labeled tripeptide (Fesik & Zuiderweg, 1988), and the feasibility of applying heteronuclear 3D NMR to small molecules at ^{13}C natural abundance has also been demonstrated (Fesik et al., 1989). Here we describe the application of a heteronuclear 3D NMR technique that is a combination of NOESY and HMQC experiments (3D NOESY–HMQC) on a dilute (0.7 mM) solution of the protein C5a (MW 8500), uniformly labeled with ^{15}N. With this technique, the NOESY spectrum of C5a is dramatically simplified, allowing cross peaks that overlap in conventional 2D NOESY spectra to be cleanly resolved. In addition to greatly facilitating the process of assigning ^1H NMR signals in crowded spectra, the improved resolution gained in the 3D NMR experiment allows more NOE cross peaks to be quantitated for purposes of 3D structure determination. Furthermore, assignments for the ^{15}N-labeled amide nitrogens, which are important for studies of protein dynamics, are easily obtained from the 3D experiment.

Experimental Procedures

^{15}N-Labeled C5a was obtained from a synthetic gene (Mandecki et al., 1985) expressed in a protease-deficient strain of *Escherichia coli* WM6 (Mandecki et al., 1986) that was grown on a minimal medium (M9) containing $^{15}NH_4Cl$ (Cambridge Isotopes) and supplemented with a broth of ^{15}N-labeled amino acids. This supplement was obtained from *E. coli* MRE 600 grown on a minimal medium containing $^{15}NH_4Cl$ and was prepared by lysing a concentrated suspension of the cells by sonication, followed by treatment with DNase, RNase, and proteinase K (Boehringer).

Uniformly ^{15}N-labeled C5a was isolated from the cell pellet by using 6 M guanidinium chloride, and the protein was subsequently allowed to refold in a 1 M solution of reduced/oxidized glutathione at pH 7.0 in 0.1 M Tris buffer. The purification of C5a was carried out by dialysis against 0.01 M HCl, which caused a large fraction of bulk protein to precipitate, followed by cation-exchange chromatography (SP-Sephadex, Pharmacia) in 20 mM formic acid (pH 5.0) with a step gradient to 0.5 M ammonium formate (pH 7.5). Further purification was obtained by gel chromatography (G75, Pharmacia) in 2% formic acid, followed by cation-exchange chromatography (SP-Sephadex, Pharmacia) with a gradient from 0 to 0.1 M sodium sulfate in a 0.01 M phosphate buffer at pH 7.

The purity of the uniformly ^{15}N-labeled C5a, which is a mixture of C5a of the native sequence and of C5a with an additional N-terminal methionine (Mandecki et al., 1985), was greater than 90% as judged from high-performance liquid chromatography, with no individual contaminant exceeding 1% of the total mass. ^{15}N isotope enrichment was found to be virtually complete. The NMR sample was prepared by dissolving 3 mg of the C5a prepared in this manner in 0.5 mL of 90% H_2O and 10% ^2H_2O for a final concentration of approximately 0.7 mM at pH 2.45.

The 3D NOESY–HMQC spectrum of C5a was recorded on a Bruker AM500 NMR spectrometer using a 5-mm ^1H broad-band inverse detection probe. The system was equipped with a X-nucleus broad-band decoupler that was phase modulated by a Smartpulse unit (Probe Systems, Champaign, IL) for a Waltz 16 sequence (Shaka et al., 1983). High-power ^{15}N pulses were obtained from the 270-W transmitter amplifier, which were combined with the broad-band decoupler output.

Solvent suppression was carried out during the 1-s relaxation delay and the NOE mixing time (0.2 s) by using a time-shared sequence (Zuiderweg et al., 1986) (200-μs delay, 3-μs pulse) with a radio-frequency power of 0.1 W; other ^1H pulses were delivered from the same ^1H decoupler amplifier at 50 W. The heteronuclear J-coupling evolution and refocusing times were 5.3 ms.

The 3D data set was collected as a series of 37 complex (t_2) data sets composed of 100 complex t_1 values and 1024 complex t_3 data points [phase sensitive (Müller & Ernst, 1979) in three dimensions]. The proton carrier was set on the H_2O resonance and the ^{15}N carrier in the center of the ^{15}N spectrum (118.9 ppm). A spectral width of $\pm$2500 Hz was used for both ω_1 and ω_3 while the spectral width in ω_2 was $\pm$500 Hz. Each acquisition consisted of 16 scans preceded by 4 dummy scans. The total actual instrument time for the 3D experiment was 177 h, of which 47 h was required for I/O operations.

A reference NOESY spectrum was recorded at 200-ms mixing time by using a 5 mM unlabeled C5a sample, pH 2.45, 20 °C. Each of the 256 complex t_1 values consisted of 64 transients of 2048 complex t_2 points with a spectral width of $\pm$5 kHz.

The NMR data were processed with in-house written software on a CSPI Minimap array processor interfaced to a Vax 8350 computer. Processing parameters are given in the caption to Figure 1. The projection of the 3D data set on the (ω_1, ω_3) plane was obtained by storing only the point of highest intensity in the ω_2 dimension at every (ω_1, ω_3) coordinate (skyline projection). The data were plotted as (ω_1, ω_3) 2D data sets at the different ω_2 (^{15}N) frequencies with the FT NMR program (Hare Research, Woodinville, WA); only positive contour levels are shown.

Results and Discussion

Figure 1A depicts a portion of a resolution-enhanced NOESY spectrum of a 5 mM solution of C5a. Although the spectrum appears to be relatively simple, detailed analysis showed that a large amount of spectral overlap occurred in the central part of the spectrum. To resolve the spectral overlap and to conduct the sequential assignments of this protein, combinations of 2D data sets were previously recorded at different experimental conditions in which the overlap patterns changed. Although this approach was possible for C5a and yielded complete assignments for the backbone protons (Zuiderweg et al., 1988), this approach was time consuming and most certainly will not be applicable for assigning the ^1H NMR spectra of larger proteins. Furthermore, the overlap of cross peaks in the NOESY spectrum of C5a made semiquantitative distance measurements impossible for many of the interesting NOE connectivities.

In order to resolve the degeneracy in amide protein resonance frequencies in the spectrum of C5a, the NOESY data set was edited with respect to the frequencies of the ^{15}N-labeled amide nitrogens in the 3D NOESY–HMQC experiment. The pulse sequence, consisting of a NOESY and a heteronuclear multiple quantum correlation (HMQC) experiment, is shown in Figure 2. As an example of coherence transfer produced by the experiment, consider proton magnetization originating on the α proton of residue i. This magnetization, which is frequency labeled during the t_1 period, can be transferred to the amide proton of residue $i + 1$ in the NOE mixing time. During the HMQC part of the experiment, this amide proton magnetization is transferred to the attached ^{15}N ($i + 1$) nucleus, where it is labeled with the ^{15}N frequency of this nucleus during t_2. The resulting coherence is transferred back to the amide proton ($i + 1$), which is detected during t_3. After 3D Fourier transformation, this sequence of events leads to a 3D cross peak at the ω_1, ω_2, ω_3 coordinates [$\Omega_{\alpha H}(i)$, $\Omega_{^{15}N}(i + 1)$,

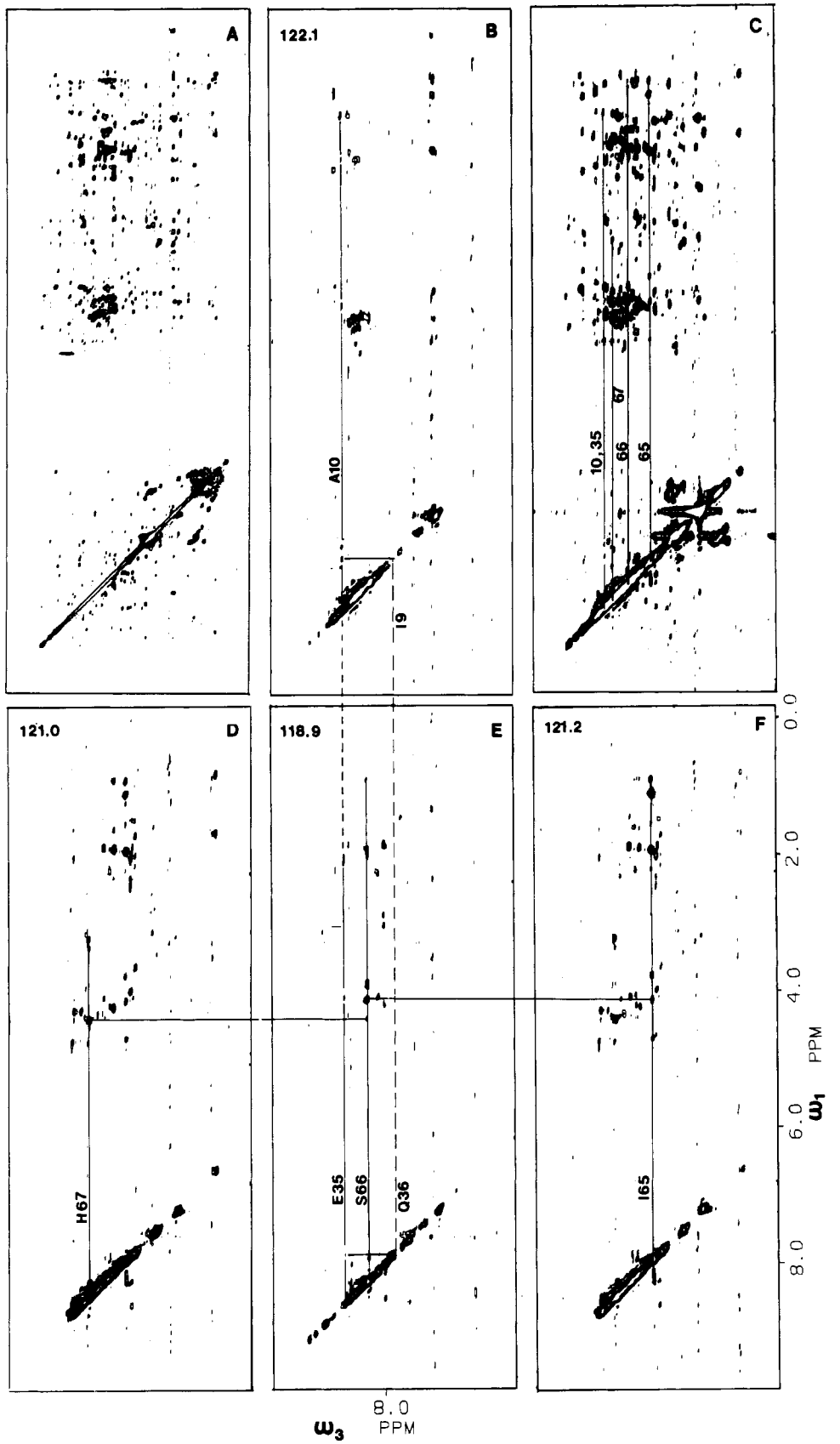

FIGURE 1: (A) Low-field region of a conventional 2D NOESY spectrum of 5 mM C5a in 90% H_2O and 10% ^2H_2O, pH 2.55, 20 °C. The data were processed with sine bell window functions shifted by 45° in both dimensions. (B, D, E, F) Cross sections through the 3D NOESY–HMQC data of 0.7 mM C5a uniformly labeled with ^{15}N in 90% H_2O and 10% ^2H_2O, pH 2.55, 20 °C. The (ω_1, ω_3) proton planes were taken at the ω_2 ^{15}N frequencies indicated in the top left corners of the panels. The data were processed with a sine bell shifted by 80°, a sine bell shifted by 90°, and exponential multiplication of 5 Hz in t_1, t_2 and t_3, respectively. Digital resolution was, after zero filling, 5, 8, and 5 Hz/point for ω_1, ω_2, and ω_3, respectively. The data were base-line corrected in ω_1 and ω_3 (unpublished software) prior to the t_2 transform. Only the low-field region of the (ω_1, ω_3) 2D data sets was transformed in t_2 for a total data size of 1024 × 128 × 384 points (ω_1, ω_2, ω_3). (C) Projection of the 3D NOESY–HMQC data on a single (ω_1, ω_3) plane.

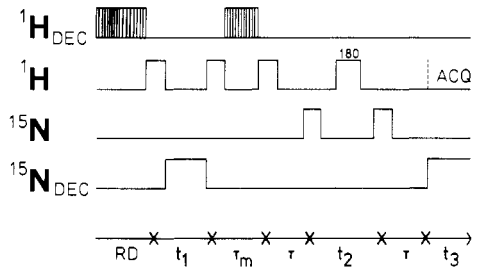

FIGURE 2: Pulse sequence of the 3D NOESY–HMQC experiment used for this study. All pulses are 90° x-phase radio-frequency pulses unless indicated otherwise. RD, τ_m, τ, and ACQ represent the relaxation delay, the NOE mixing time, the heteronuclear coupling evolution and refocusing time, and data acquisition, respectively. A 16-step phase cycling scheme in which the first proton pulse, the proton 180° pulse, and both ^{15}N pulses were independently inverted with appropriate receiver phase inversions was employed. Quadrature detection (Müller & Ernst, 1977) was used in all time domains.

$\Omega_{NH}(i + 1)$]. The resulting 3D FT data set of this sequence can thus be viewed as a stack of NOESY spectra edited with respect to the ^{15}N frequencies with the full ^1H NMR spectral width in ω_1, ^{15}NH resonances in ω_2, and ^{15}N*H* in ω_3.

Parts B, D, E, and F of Figure 1 show a few of the (ω_1, ω_3) NOESY planes from the 3D NOESY–HMQC experiment conducted with uniformly ^{15}N-enriched C5a (0.7 mM), together with a projection of the entire 3D data set on a single plane (Figure 1C). It is seen that the individual ^1H–^1H NOESY planes contain only a few signals, thus greatly facilitating the interpretation of overlapping resonances occurring in the 2D data. A large resolution improvement is obtained for the crowded fingerprint region of the NOESY spectrum, which contains the intra- and interresidue NOE connectivities ($d_{\alpha N}$) between α protons (ω_1 = 4–5 ppm) and amide protons (ω_3 = 6–9 ppm). For example, it is seen in Figure 1D that the NOE responses of the His-67 amide proton are completely resolved in the 3D data (ω_2 = 121.0 ppm). The strong cross peak in the fingerprint region, which is masked by other signals in the 2D data, is totally resolved in the 3D data set and can easily be assigned to the sequential connectivity $d_{\alpha N}(i, i + 1)$ involving Ser-66 (Figure 1E). The connectivity pathway can be followed further in the ^{15}N plane corresponding to the amide nitrogen of Ser-66 (118.9 ppm) in which a strong $d_{\alpha N}(i, i + 1)$ connectivity leads to Ile-65 αH (Figure 1E,F). In the conventional NOESY spectrum, analysis of this connectivity is also severely hampered by spectral overlap (see Figure 1A,C).

Another example of the utility of the 3D experiment for resolving overlapping NOE cross peaks is shown in the amide region for Ala-10 NH (Figure 1B, ω_2 = 122.1 ppm). In addition to the intraresidue cross peaks CαH–NH and CβH_3–NH, two amide proton–amide proton (d_{NN}) cross peaks are unambiguously identified to belong to Ala-10 NH. These latter cross peaks are assigned to Ile-9 NH–Ala-10 NH and Ala-11 NH–Ala-10 NH and are also clearly visible in the 2D data and in the projection (Figure 1C). However, another d_{NN} cross peak contributes to the intensity of the Ile-9–Ala-10 connectivity. This cannot be resolved in the 2D data but is clearly revealed in the 3D data in the plane at ^{15}N frequency 118.9 ppm. From an analysis of the data this was found to be the sequential d_{NN} NOE between Glu-35 and Gln-36, which resonates at the same (ω_1, ω_3) coordinates as the Ile-9 NH–Ala-10 NH connectivity as indicated in the figure. Thus, the 3D experiment resolved the cross-peak overlap occurring at these coordinates and allowed the unambiguous assignment of the cross peaks to particular amide protons.

As indicated by these examples, proton assignments are greatly facilitated by the 3D NOESY–HMQC experiment. Unlike in 2D spectra, cross-peak overlap is largely eliminated in 3D, making it extremely easy to recognize the spin systems in the individual ^{15}N planes. For example, the pattern obtained for His-67 (Figure 1D) in the 3D data strongly indicates an AMX spin system, while such an identification is impossible in the 2D data (see Figure 1C). This spin system recognition is of great importance for the assignment procedure (Wüthrich, 1986). From the 3D data a large amount of sequential connectivities were found (Figure 3). As indicated in this figure, many d_{NN} and $d_{\alpha N}(i, i + 1)$ connectivities could be detected in this α-helical protein. Even some weak NOEs corresponding to distances of 3.5 Å [e.g., $d_{\alpha N}(i, i + 1)$ NOEs in α-helical regions] could be observed. Thus, the majority of the ^1H assignments in C5a could be made from this 3D data set. Furthermore, no discrepancies were found when compared with the published data (Zuiderweg et al., 1988). Interruptions in the assignment diagram were caused by bleaching of $d_{\alpha N}(i, i + 1)$ NOEs due to solvent suppression or by overlap of amide proton resonances of residues adjacent in the sequence in

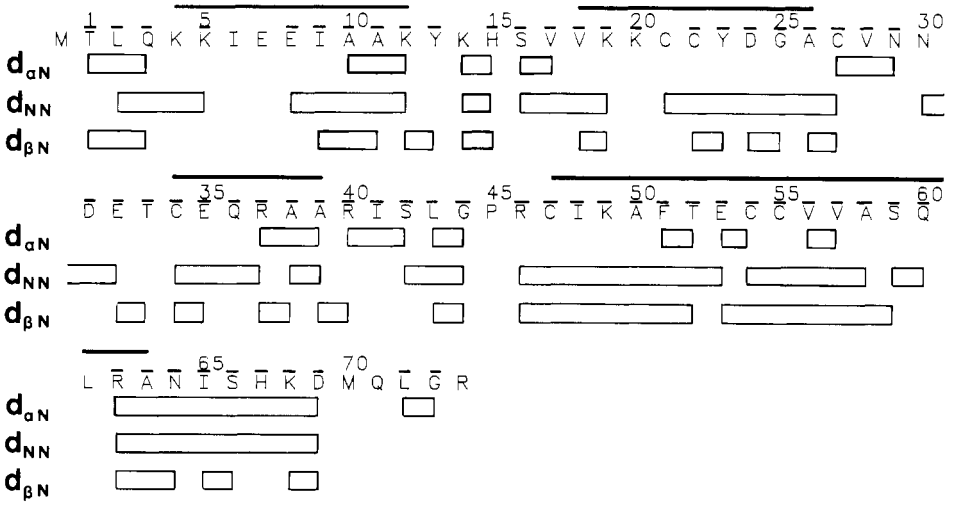

FIGURE 3: Overview of the sequential connectivities obtained from analysis of the 3D NOESY–HMQC data. The symbol $d_{\alpha N}$ represents an NOE between the α proton of residue i and the amide proton of residue $i + 1$; the symbol d_{NN} represents an NOE between the amide protons of sequentially adjacent residues; the symbol $d_{\beta N}$ represents an NOE between the β proton of residue i and the amide proton of residue $i + 1$. Amide nitrogens for which ^{15}N resonance assignments were obtained are indicated with a small bar above the amino acid residue symbol. The locations of α helices in C5a (Zuiderweg et al., 1989) are shown by the solid bars above the sequence.

α-helical regions of the protein. In this latter case, the expected d_{NN} coincides with the amide proton diagonal, a spectral overlap situation that cannot be resolved by the 3D NOESY–HMQC technique.

The completeness of the 3D data obtained from the NOESY–HMQC experiment is especially remarkable if one considers that the experiment was carried out with a very dilute sample (0.7 mM). As expected, the individual ^{15}N-filtered NOESY spectra, which were acquired in only 2 h, are of very marginal quality. However, a very substantial sensitivity increase is obtained by recording many of these 2D data as a function of the ^{15}N evolution time in a third dimension, a process totally analogous to that occurring in 2D NMR as compared to 1D NMR. Moreover, window functions emphasizing sensitivity rather than resolution are used for the processing of the 3D data; resolution is obtained from the third dimension in these experiments. While these considerations hold true for all 3D experiments, it is the special advantage of heteronuclear 3D NMR over homonuclear 3D NMR that coherence transfer involves a large heteronuclear coupling that allows efficient correlation with very little loss for larger systems.

Apart from facilitating the assignment procedure as described above, the increase in resolution obtained in the 3D experiment also allows the semiquantitative determination of NOE cross-peak volumes in otherwise overlapping spectral regions. The additional intra- and interresidue distance constraints between amide protons and side-chain protons obtained from such measurements in the 3D NOESY–HMQC data are of great value for more precise tertiary structure determinations of proteins. Examples of this are shown in parts B and D of Figure 1, where the NOEs Ala-10 NH–Ile-9 CβH and Ser-66 NH–Ile-65 side chain, respectively, have become accessible for cross-peak integration.

Another application of the 3D NOESY–HMQC experiment is to facilitate the assignments of ^{15}N signals. ^{15}N NMR assignments are important for interpreting individual ^{15}N relaxation times used in the study of protein dynamics. Since ^{15}N assignments are obtained from proton assignments, overlap in the latter results in ambiguity for the ^{15}N signal identification. These ambiguities cannot be resolved in a two-dimensional HMQC experiment. However, in the 3D NOESY–HMQC spectrum, which may be viewed as an editing technique for HMQC data, the assignment of ^{15}N resonances is greatly facilitated. From the 3D NOESY–HMQC spectrum many of the ^{15}N resonances of C5a were assigned. The assigned signals are indicated in Figure 3, and a listing is available as supplementary material (see paragraph at end of paper regarding supplementary material).

In conclusion, we have demonstrated that a large improvement in resolution is obtained for the amide proton NOESY spectrum of C5a using the 3D NOESY–HMQC technique. The enhanced resolution will facilitate the ^1H NMR assignments in larger proteins and will also aid in the semiquantitative determination of cross-peak volumes in congested parts of NOESY spectra. In addition, ^{15}N resonance assignments are easily obtained from this experiment, which are important for the study of protein dynamics. Finally, it is demonstrated that heteronuclear 3D NMR spectroscopy is a practical technique since only relatively small quantities of labeled protein are necessary for the experiment (3 mg for C5a). These features suggest that ^{15}N heteronuclear 3D NMR will become a routine tool for facilitating the spectral analysis of smaller molecules while the technique provides novel possibilities for the study of (much) larger systems that thus far could not be investigated in detail by NMR.

Acknowledgments

We thank Dr. W. Mandecki, K. W. Mollison, M. Seavy, M. A. Shallcross, Dr. C. B. Credo, R. P. Edalji, and R. T. Gampe, Jr., for advice and assistance with the ^{15}N protein expression and purification.

Supplementary Material Available

One table listing the ^{15}N chemical shifts of the amide nitrogens of C5a at pH 2.45, 20 °C (1 page). Ordering information is given on any current masthead page.

Registry No. C5a, 80295-54-1.

References

Bax, A., Griffey, R. H., & Hawkins, B. L. (1983) *J. Magn. Reson. 55*, 301.

Bax, A., Clore, G. M., Driscoll, P., Gronenborn, A. M., Ikura, M., Kay, L., Marion, D., Sparks, S., & Torchia, D. A. (1988) XIIIth International Conference on Magnetic Resonance in Biological Systems, Madison, WI.

Ernst, R. R., Bodenhausen, G., & Wokaun, A. (1987) *Principles of nuclear magnetic resonance in one and two dimensions*, Clarendon Press, Oxford, U.K.

Fesik, S. W., & Zuiderweg, E. R. P. (1988) *J. Magn. Reson. 78*, 588.

Fesik, S. W., Gampe, R. T., Jr., & Zuiderweg, E. R. P. (1989) *J. Am. Chem. Soc. 111*, 770.

Griesinger, C., Sørensen, O. W., & Ernst, R. R. (1987a) *J. Magn. Reson. 73*, 574.

Griesinger, C., Sørensen, O. W., & Ernst, R. R. (1987b) *J. Am. Chem. Soc. 109*, 7227.

Mandecki, W., Mollison, K. W., Bolling, T. J., Powell, B. S., Carter, G. W., & Fox, J. L. (1985) *Proc. Natl. Acad. Sci. U.S.A. 82*, 3543.

Mandecki, W., Powell, B. S., Mollison, K. W., Carter, G. W., & Fox, J. L. (1986) *Gene 43*, 131.

Müller, L. (1979) *J. Am. Chem. Soc. 101*, 4481.

Müller, L., & Ernst, R. R. (1979) *Mol. Phys. 38*, 963.

Oschkinat, H., Griesinger, C., Kraulis, P. J., Sørensen, O. W., Ernst, R. R., Gronenborn, A. M., & Clore, G. M. (1988) *Nature 332*, 374.

Shaka, A. J., Keeler, J., Frenkiel, T., & Freeman, R. (1983) *J. Magn. Reson. 52*, 335.

Vuister, G. W., & Boelens, R. (1987) *J. Magn. Reson. 73*, 328.

Vuister, G. W., Boelens, R., & Kaptein, R. (1988) *J. Magn. Reson. 80*, 176.

Wüthrich, K. (1986) *NMR of Proteins and Nucleic Acids*, Wiley, New York.

Zuiderweg, E. R. P., Hallenga, K., & Olejniczak, E. T. (1986) *J. Magn. Reson. 70*, 336.

Zuiderweg, E. R. P., Mollison, K. W., Henkin, J., & Carter, G. W. (1988) *Biochemistry 27*, 2568.

Zuiderweg, E. R. P., Nettesheim, D. G., Mollison, K. W., & Carter, G. W. (1989) *Biochemistry 28*, 172.